Electronic Supplementary Material (ESI) for Analyst.

Supplementary Information

NIR-Emitting Benzene-Fused Oligo-BODIPYs for Bioimaging

*Gabriele Selvaggio[1,2,†], Robert Nißler[1,2,†], Peter Nietmann[2], Lukas J. Patalag[3], Atanu Patra[3], Andreas Janshoff[2], Daniel B. Werz[3], Sebastian Kruss[1,2,4]**

[1]Physical Chemistry II, Bochum University, Bochum, 44801, Germany

[2]Institute of Physical Chemistry, University of Göttingen, Göttingen, 37077, Germany

[3]Institute of Organic Chemistry, Technical University of Braunschweig, Braunschweig, 38106, Germany

[4]Fraunhofer Institute for Microelectronic Circuits and Systems, Duisburg, 47057, Germany

†These authors contributed equally.

*Corresponding author: sebastian.kruss@rub.de

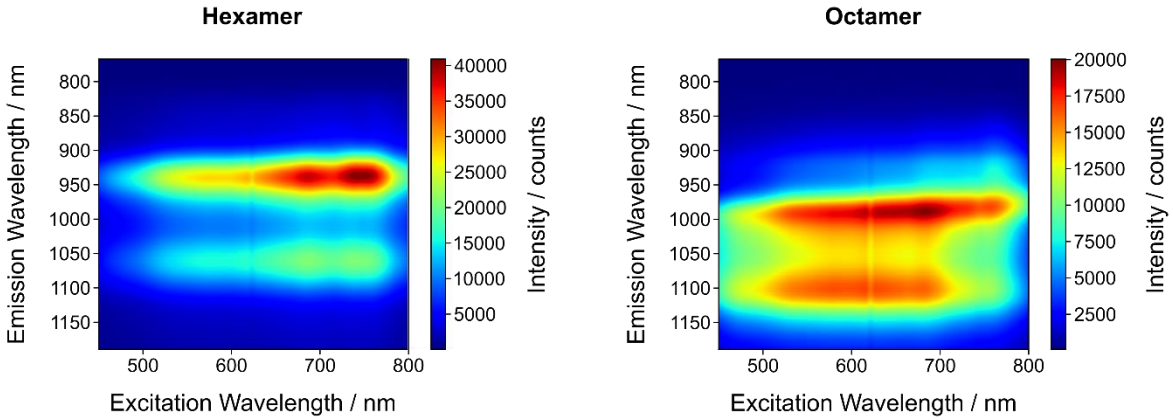

Figure S1: 2D spectra of NIR dyes. *2D excitation-emission spectra of the hexamer and octamer NIR dyes. Due to the cut-on wavelength of the dichroic mirror in our setup, the emission features resulting from excitation wavelengths > 800 nm are not measured. Therefore, the maxima for both hexamer and octamer samples are not observable.*

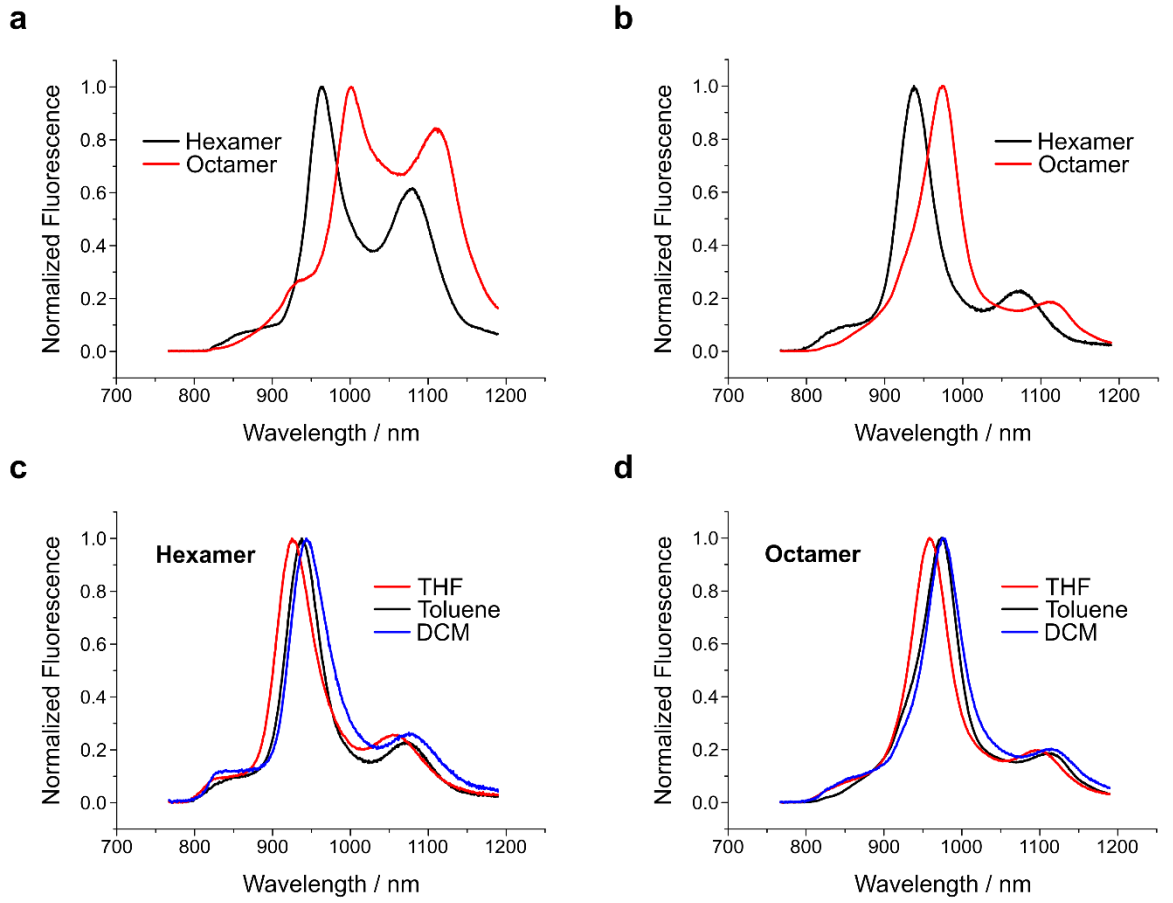

Figure S2: Concentration effects and solvatochromism. ***a*** *Normalized fluorescence emission of highly concentrated samples (≈ 5 µM) of hexamer and octamer in dichloromethane (DCM).* ***b*** *Normalized fluorescence emission of diluted samples (≈ 0.5 µM) of hexamer and octamer in DCM show an altered ratio of the two largest peaks, as well as a hypsochromic shift and peak broadening, compared to more concentrated batches.* ***c*** *Solvent-dependent peak shifts in the emission profile of the hexamer-BODIPY in tetrahydrofuran (THF), toluene and DCM.* ***d*** *Solvent-dependent peak shifts in the emission profile of the octamer-BODIPY in THF, toluene and DCM.*

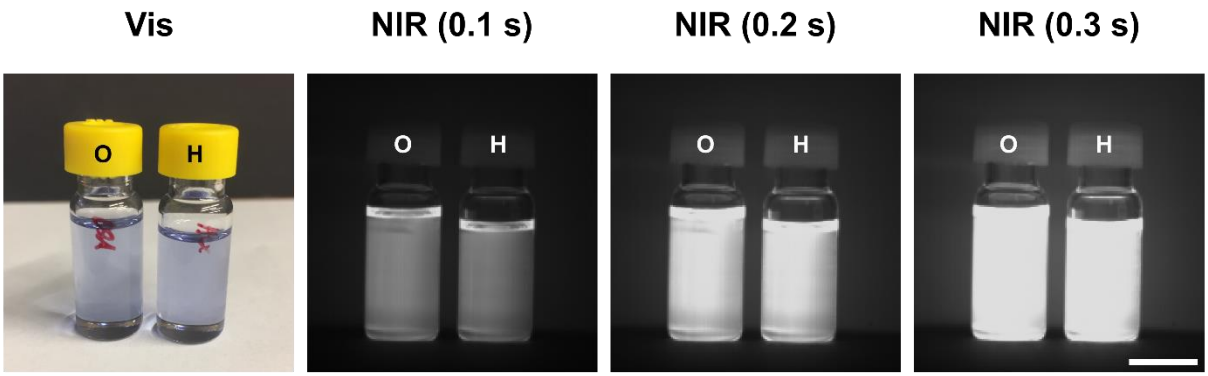

Figure S3: Stand-off NIR images of highly concentrated octamer- (O) and hexamer- (H) BODIPYs. *NIR fluorescence images of highly concentrated solutions (≈ 5 µM) of octamer and hexamer dyes in toluene. Acquisition was performed with our home-built stand-off setup at maximum illumination power and at different exposure times: while t = 0.1 s is already sufficient to notice the bright fluorescence of the samples, with t = 0.3 s pixel saturation of the NIR camera starts becoming observable. Scale bar = 1 cm.*

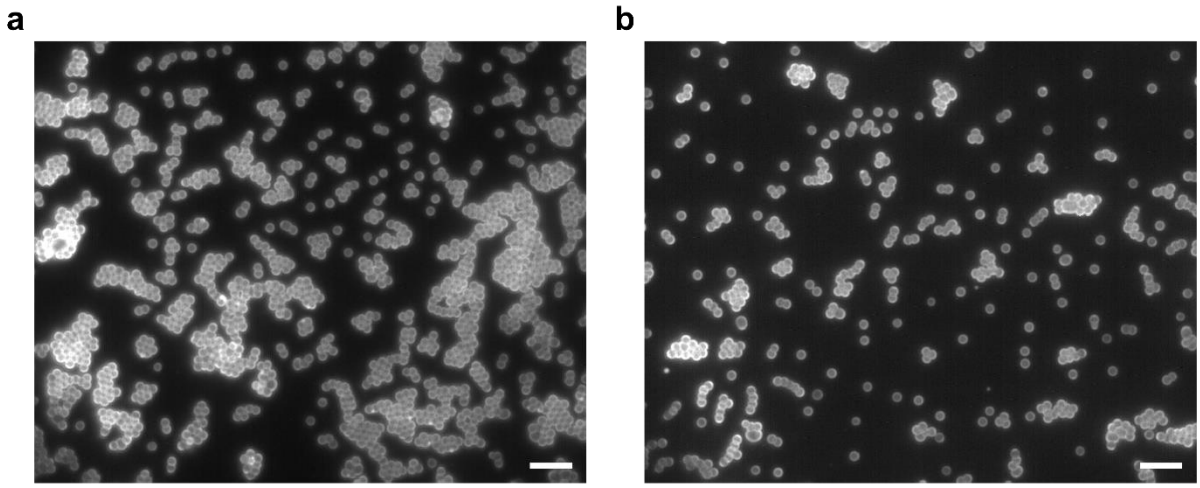

Figure S4: NIR images of hexamer-coated lower-size PS beads. *NIR fluorescence images of higher (**a**) and lower (**b**) concentrations of PS beads with diameter ≈ 1.5 µm. These beads were tracked in actin networks of different concentrations thanks to their NIR fluorescent coating. Scale bar = 10 µm.*

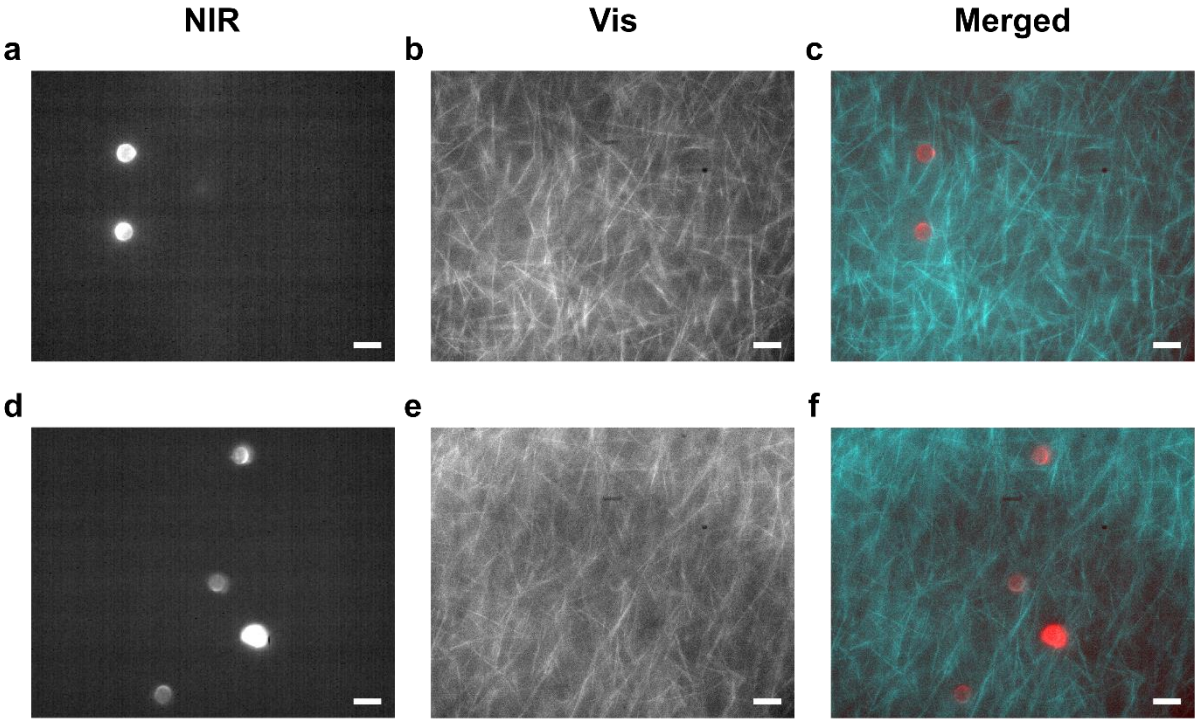

Figure S5: Coating of the hexamer-BODIPY dye on silica beads and dual-color imaging in actin networks. *Besides the PS beads, also plain silica beads of diameter ≈ 6 µm were successfully coated and embedded into actin filaments, proving the versatility of the NIR dye. Different imaging channels (**a**-**c**, **d**-**f**) are shown: NIR (**a**,**d**) for detection of the hexamer-BODIPY, Vis (**b**,**e**) for detection of the actin filaments labelled with a Vis dye, and the merging of the channels in false colors (**c**,**f**) for co-localization. Scale bar = 10 µm.*

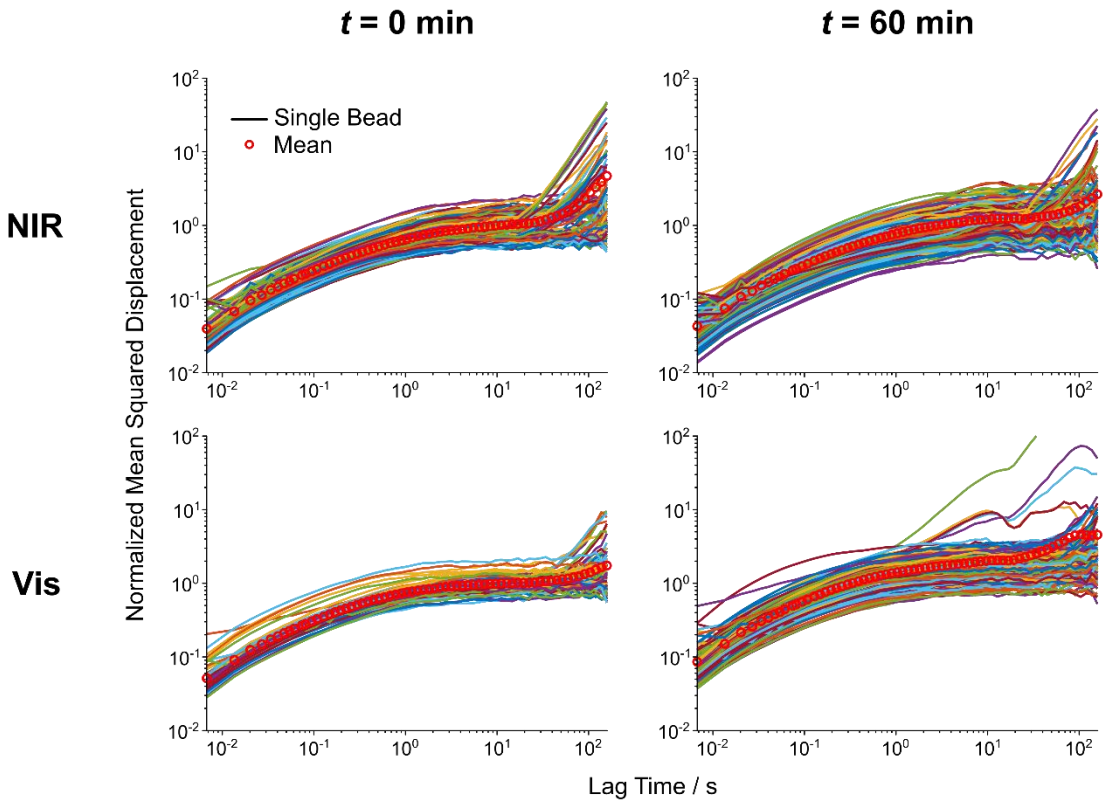

Figure S6: Single mean squared displacement (MSD) curves for actin degradation experiments. *Single (colored lines) and mean (red circles) MSD curves resulting from video-particle tracking (VPT) of PS beads in actin networks after 60 min of continuous illumination. PS microspheres coated either with our NIR hexamer-BODIPY (NIR) or with a commercially available visible (Vis) dye (fluorescent red PS microspheres, 545/566 nm, FRP5000, Lab 261) were employed for this study. The 60 min datasets were normalized to the respective 0 min MSD at lag time = 10 s (i.e. in the middle of the plateau region). For the NIR dataset, n = 114 beads at t = 0 min and 169 beads at t = 60 min. For the Vis dataset, n = 103 beads at t = 0 min and 184 beads at t = 60 min. N = 5 independent samples.*

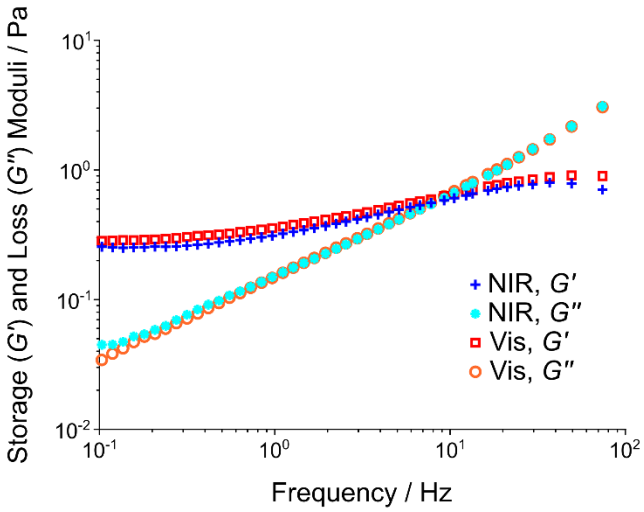

Figure S7: Storage and loss moduli for actin degradation experiments. *Storage (G') and loss (G'') moduli for both visible (Vis) and near-infrared (NIR) beads tracked in an actin network for 60 min under continuous illumination. The shown data corresponds to t = 0 min.*

Table S1: Emission features of hexamer (H) and octamer (O) benzene-fused oligo-BODIPYs at high concentrations. *The first ($\lambda_{em,1}$) and second ($\lambda_{em,2}$) emission peaks as well as the respective full widths at half maximum ($FWHM_{em,1}$ and $FWHM_{em,2}$) of highly concentrated ("high", ≈ 5 µM) dye samples in dichloromethane (DCM) are reported.*

Sample	$\lambda_{em,1\ (high)}$ / nm (cm^{-1})	$FWHM_{em,1\ (high)}$ / nm (cm^{-1})	$\lambda_{em,2\ (high)}$ / nm (cm^{-1})	$FWHM_{em,2\ (high)}$ / nm (cm^{-1})
H	963 (10389)	62.6 (408.7)	1080 (9260)	93.0 (828.6)
O	1002 (9985)	68.2 (637.6)	1108 (9009)	134.7 (1069.9)

Table S2: Emission features of hexamer (H) and octamer (O) benzene-fused oligo-BODIPYs at low concentrations. *The first ($\lambda_{em,1}$) and second ($\lambda_{em,2}$) emission peaks as well as the respective full widths at half maximum ($FWHM_{em,1}$ and $FWHM_{em,2}$) of diluted ("low", ≈ 0.5 µM) dye samples in dichloromethane (DCM) are reported.*

Sample	$\lambda_{em,1\ (low)}$ / nm (cm^{-1})	$FWHM_{em,1\ (low)}$ / nm (cm^{-1})	$\lambda_{em,2\ (low)}$ / nm (cm^{-1})	$FWHM_{em,2\ (low)}$ / nm (cm^{-1})
H	938 (10667)	49.6 (579.5)	1074 (9315)	98.1 (1177.6)
O	974 (10264)	56.0 (594.2)	1108 (9022)	125.0 (931.3)

Table S3: Solvatochromism of hexamer (H) and octamer (O) benzene-fused oligo-BODIPYs. *The first ($\lambda_{em,1}$) and second ($\lambda_{em,2}$) emission peaks of the dyes dissolved in tetrahydrofuran (THF), toluene and dichloromethane (DCM) are reported.*

Sample	$\lambda_{em,1\ (THF)}$ / nm (cm^{-1})	$\lambda_{em,2\ (THF)}$ / nm (cm^{-1})	$\lambda_{em,1\ (toluene)}$ / nm (cm^{-1})	$\lambda_{em,2\ (toluene)}$ / nm (cm^{-1})	$\lambda_{em,1\ (DCM)}$ / nm (cm^{-1})	$\lambda_{em,2\ (DCM)}$ / nm (cm^{-1})
H	925 (10813)	1054 (9485)	938 (10667)	1074 (9315)	943 (10601)	1075 (9301)
O	958 (10434)	1097 (9113)	974 (10264)	1115 (9022)	976 (10247)	1115 (8971)